

RESEARCH ARTICLE | JUNE 15 2023

Mesoscale computer modeling of asphaltene aggregation in liquid paraffin

Andrey A. Gurtovenko  ; Victor M. Nazarychev ; Artem D. Glova ; Sergey V. Larin ;
Sergey V. Lyulin 



J. Chem. Phys. 158, 234902 (2023)

<https://doi.org/10.1063/5.0153741>



View
Online



Export
Citation

CrossMark



The Journal of Chemical Physics
Special Topic: Adhesion and Friction

Submit Today!



Mesoscale computer modeling of asphaltene aggregation in liquid paraffin

Cite as: *J. Chem. Phys.* **158**, 234902 (2023); doi: 10.1063/5.0153741

Submitted: 11 April 2023 • Accepted: 30 May 2023 •

Published Online: 15 June 2023



View Online



Export Citation



CrossMark

Andrey A. Gurtovenko,^{1,a)}  Victor M. Nazarychev,¹  Artem D. Glova,²  Sergey V. Larin,¹ 
and Sergey V. Lyulin¹ 

AFFILIATIONS

¹Institute of Macromolecular Compounds, Russian Academy of Sciences, Bolshoi Prospect V.O. 31, St. Petersburg 199004, Russia

²Department of Physics and Astronomy, The University of Western Ontario, 1151 Richmond Street, London, Ontario N6A 3K7, Canada

^{a)} Author to whom correspondence should be addressed: a.gurtovenko@biosimu.org

ABSTRACT

Asphaltenes represent a novel class of carbon nanofillers that are of potential interest for many applications, including polymer nanocomposites, solar cells, and domestic heat storage devices. In this work, we developed a realistic coarse-grained Martini model that was refined against the thermodynamic data extracted from atomistic simulations. This allowed us to explore the aggregation behavior of thousands of asphaltene molecules in liquid paraffin on a microsecond time scale. Our computational findings show that native asphaltenes with aliphatic side groups form small clusters that are uniformly distributed in paraffin. The chemical modification of asphaltenes via cutting off their aliphatic periphery changes their aggregation behavior: modified asphaltenes form extended stacks whose size increases with asphaltene concentration. At a certain large concentration (44 mol. %), the stacks of modified asphaltenes partly overlap, leading to the formation of large, disordered super-aggregates. Importantly, the size of such super-aggregates increases with the simulation box due to phase separation in the paraffin–asphaltene system. The mobility of native asphaltenes is systematically lower than that of their modified counterparts since the aliphatic side groups mix with paraffin chains, slowing down the diffusion of native asphaltenes. We also show that diffusion coefficients of asphaltenes are not very sensitive to the system size: enlarging the simulation box results in some increase in diffusion coefficients, with the effect being less pronounced at high asphaltene concentrations. Overall, our findings provide valuable insight into the aggregation behavior of asphaltenes on spatial and time scales that are normally beyond the scales accessible for atomistic simulations.

Published under an exclusive license by AIP Publishing. <https://doi.org/10.1063/5.0153741>

I. INTRODUCTION

Asphaltenes represent one of the heaviest aromatic fractions of crude oil.¹ Asphaltene molecules readily aggregate, which makes them responsible for the increased oil viscosity, plugging of pipelines, and equipment downtime.^{2–5} Due to its negative economic impact, an asphaltene fraction is normally extracted from crude oil, so asphaltenes can be considered low-cost side products of deep oil refining. Besides petroleum, asphaltene molecules can also be isolated from ethylene tar, a side product of ethylene production.⁶

As such, asphaltenes are defined as aromatic compounds that are soluble in toluene and insoluble in *n*-heptane.^{1,7} Although this definition is applicable to a vast variety of molecular architectures, most asphaltene molecules consist of a relatively small

polycyclic aromatic core (more rarely, several cores) decorated with short alkane chains.¹ The polycyclic planar cores of asphaltenes can interact via π – π interactions that most likely govern asphaltene aggregation.^{8,9}

Recently, due to their abundance, ability to aggregate, and low cost, asphaltene molecules have attracted attention as a promising class of carbon nanofillers. In particular, asphaltenes were used to improve the thermal and mechanical properties of polymer and epoxy nanocomposites.^{10–12} The electronic conductivity of asphaltenes inspired attempts to probe them as acceptor materials for bulk heterojunction solar cells.¹³ Last but not least, asphaltenes were proposed to be used as non-expensive carbon nanofillers to enhance the thermal conductivity of organic phase-change materials such as paraffin.^{6,14,15} For most of the above-mentioned applications, it is highly desirable to promote the stacking of asphaltene

molecules, which can be achieved by reducing the fraction of peripheral aliphatic chains in asphaltene molecules,^{16–18} thereby enhancing the π - π interactions between asphaltene's polycyclic aromatic cores. As far as organic phase-change materials are concerned, extended stacks of asphaltenes can form thermal conduction paths, thereby accelerating heat transfer. Indeed, as demonstrated in Ref. 6, an appropriate chemical modification aimed at removing the asphaltene's aliphatic side chains made it possible to considerably increase (by 72%) the thermal conductivity of paraffin-asphaltene composite systems.

Remarkably, similar effects were also observed in our recent atomistic computer simulations of paraffin samples filled with asphaltene molecules.¹⁹ One of the advantages of computer modeling is that it provides precise control over the chemical structure of asphaltene molecules at hand; unlike experimental methods, simulations allow one to completely cut off the aliphatic periphery of asphaltenes. Correspondingly, computer simulations showed that adding asphaltenes with aliphatic chains cut off to liquid paraffin could drastically enhance the thermal conductivity of the resulting composite systems.¹⁹ It is also noteworthy that the relatively small polycyclic aromatic cores of asphaltenes resemble model polyaromatic hydrocarbons (such as coronene or ovalene) that form discotic liquid crystals.^{20,21} Therefore, studying the aggregation of modified asphaltenes without aliphatic periphery could also shed light on the packing properties of discotic liquid crystalline molecules.

Although atomistic computer modeling provides unprecedented insight into the microscopic structure and properties of molecular systems, it has obvious limitations regarding the time and length scales accessible. In particular, the impact of system size on the details of asphaltene aggregation is still an open question.²² Indeed, most published atomistic simulation studies were limited to the systems of a hundred asphaltene molecules, which were normally simulated over several hundred nanoseconds at best.^{23–28} A way forward is to employ coarse-grained models;^{29–33} they allow one to probe larger systems for longer periods, provided that most molecular details of the system at hand are well preserved.

In this paper, we develop a realistic coarse-grained model for studying the aggregation behavior of asphaltene molecules in liquid paraffin. The model was based on the Martini force field that has been successfully applied for mesoscale simulations of various carbon nano-objects such as fullerenes,³⁴ carbon nanotubes,^{35,36} graphene,^{37,38} bitumen,³⁹ and asphaltenes.³⁰ Furthermore, the Martini model was extensively validated for the description of liquid *n*-alkanes.^{40,41} Our coarse-grained model was refined against atomistic simulation data (the free energy of asphaltene dimerization). This allowed us for the first time to follow the aggregation of thousands of asphaltene molecules in paraffin at a near-atomistic resolution on a microsecond time scale. The outcome of the mesoscopic simulations was systematically compared to the computational results obtained independently with the use of two different full-atom force fields. In particular, our mesoscale simulations made it possible to identify which physical properties of paraffin-asphaltene systems should be considered with caution due to finite-size effects and phase separation.

II. METHODS

A. Coarse-grained simulations

We performed coarse-grained molecular dynamics simulations of paraffin filled with asphaltene molecules. A short-chain alkane, *n*-eicosane ($C_{20}H_{42}$), was used to mimic paraffin. As for asphaltenes, we considered a model asphaltene molecule with seven fused aromatic rings and one sulfur heteroatom, which was decorated by several alkane side fragments,^{1,42–45} see Fig. 1(a). This asphaltene molecule complies with the solubility/insolubility definition of asphaltenes²⁸ as well as with the typical molecular architecture of petroleum asphaltenes according to experimental data (one polyaromatic core with on average seven fused rings).¹ Importantly, this choice of system allows us to perform a direct comparison of the outcome of mesoscale simulations with the atomic-scale simulation data available for the same system.¹⁹

To access the aggregation behavior of thousands of asphaltene molecules in the paraffin matrix, the coarse-grained (CG) Martini force field (version 2.2) was employed.^{46–48} According to the standard Martini representation, four CH_2 groups of paraffin chains and aliphatic side fragments of asphaltenes were represented by a single C1 bead, while three SC5 coarse-grained beads were used to describe an aromatic ring of the asphaltene's core;^{46,47} see Fig. 1 for mapping details. The standard masses of the C1 and SC5 Martini beads were reduced to 56 and 25, respectively, to match the actual masses of the corresponding atomic groups. The Martini mapping resulted in a considerable reduction in the number of interaction sites compared to the atomistic representation: 5 CG beads vs 62 atoms for *n*-eicosane, 21 CG beads vs 114 atoms for asphaltenes, and 14 CG beads vs 39 atoms for asphaltene's cores (or modified asphaltenes).

Two sets of systems were studied. The first set consisted of 500 paraffin molecules and (from 21 to 396) asphaltenes and coincided with the systems considered in our earlier atomistic computational

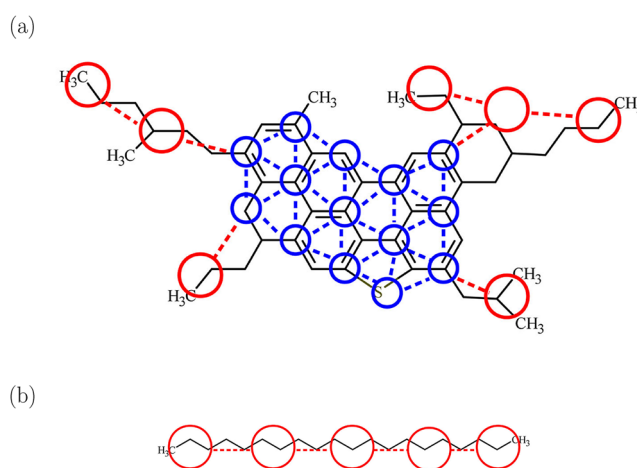


FIG. 1. The chemical structure and mapping of a model asphaltene molecule (a) and a paraffin chain (b). Coarse-grained C1 beads are denoted by red circles, while SC5 beads are denoted by blue circles.

study.¹⁹ This allowed us to perform a direct comparison of coarse-grained and atomistic simulations of paraffin samples filled with asphaltenes. The second set contained much larger systems, in which the number of molecules was increased by a factor of 10. Similar to Ref. 19, to get insight into the impact of aliphatic side chains on the aggregation behavior of asphaltenes, all the simulations were repeated twice with native asphaltenes (PAR-ASP systems) and with modified asphaltenes with the aliphatic periphery cut off (PAR-ASPM systems). All studied coarse-grained systems are listed in Table I.

The Lennard-Jones interactions were cut off at 1.1 nm.⁴⁹ The systems were simulated in the NpT ensemble at $p = 1$ bar and $T = 450$ K. The pressure was controlled isotropically with the Parrinello–Rahman barostat⁵⁰ (a coupling constant of 20 ps). To control temperature, we employed a velocity-rescaling thermostat⁵¹ with a coupling constant of 1 ps. The time step was set to 20 fs. Each system listed in Table I was simulated for 1 μ s. All simulations were performed using the Gromacs suite (v. 2018.6).^{52,53}

The temperature of 450 K was chosen to be well above the phase transition temperature of *n*-eicosane (310 K)⁵⁴ so that the simulated systems were in the liquid state. It has to be emphasized that in the Martini representation, *n*-eicosane does not crystallize when the temperature drops below the transition temperature. To demonstrate that, we cooled down the *n*-eicosane sample (the PAR system in Table I) in a stepwise manner from 450 to 200 K at a cooling rate of 6×10^9 K/min.⁵⁵ Our cooling-rate computer simulations showed a lack of an abrupt change in the temperature dependence of the *n*-eicosane mass density in Martini simulations, which was observed

TABLE I. Simulated coarse-grained systems. Shown are the number of paraffin molecules, N_{par} ; the number of asphaltenes, N_{asph} ; the molar concentration of asphaltenes, C_{asph} ; and the total number of beads, N_{beads} .

System	N_{par}	N_{asph}	C_{asph} (mol. %)	N_{beads}
PAR	500	2 500
PAR-ASP-4	500	21	4	2 941
PAR-ASP-8	500	44	8	3 424
PAR-ASP-17	500	99	17	4 579
PAR-ASP-30	500	214	30	6 994
PAR-ASP-44	500	396	44	10 816
PAR-ASPM-4	500	21	4	2 794
PAR-ASPM-8	500	44	8	3 116
PAR-ASPM-17	500	99	17	3 886
PAR-ASPM-30	500	214	30	5 496
PAR-ASPM-44	500	396	44	8 044
PAR-Large	5000	25 000
PAR-ASP-4-Large	5000	210	4	29 410
PAR-ASP-8-Large	5000	440	8	34 240
PAR-ASP-17-Large	5000	990	17	45 790
PAR-ASP-30-Large	5000	2140	30	69 940
PAR-ASP-44-Large	5000	3960	44	108 160
PAR-ASPM-4-Large	5000	210	4	27 940
PAR-ASPM-8-Large	5000	440	8	31 160
PAR-ASPM-17-Large	5000	990	17	38 860
PAR-ASPM-30-Large	5000	2140	30	54 960
PAR-ASPM-44-Large	5000	3960	44	80 440

in experiments^{56,57} and atomistic simulations,^{58,59} see Fig. S1. However, this finding agrees with Ref. 60, where a similar behavior was also witnessed in coarse-grained simulations of polyethylene, provided that the mapping was 4:1 or coarser. In particular, this implies that the Martini force field is applicable only to studying liquid paraffin, which is the subject of our study.

Since our preliminary test simulations showed that the standard Martini force field considerably overestimates the asphaltene aggregation, the interaction parameters for SC5–SC5 (asphaltene core–asphaltene core) and SC5–C1 (asphaltene core–paraffin) pairs were fine-tuned. To this end, we used the free energy (the potential of mean force, PMF) of asphaltene dimerization and adjusted it to the PMF profile evaluated from atomistic simulations; see Sec. III A for details. To calculate the free energy of asphaltene dimerization, the umbrella sampling technique was used.⁶¹ As the aromatic cores of asphaltenes are mainly responsible for their aggregation, we focused on the interactions of two modified asphaltene molecules without aliphatic side chains in liquid paraffin. The system consisted of two modified asphaltenes and 140 *n*-eicosane chains (728 CG beads in total). We generated 18 configurations (windows), with the distance between the centers of mass of the asphaltenes varying from 0.3 to 2.0 nm with a step of 0.1 nm. Each umbrella window was simulated for 100 ns with a force constant of $1000 \text{ kJ mol}^{-1} \text{ nm}^{-2}$, and the last 60 ns of trajectories were used for computing the PMF by the weighted histogram analysis (WHAM) method.^{62,63} We also repeated the PMF calculations in vacuum with an increased force constant of $2000 \text{ kJ mol}^{-1} \text{ nm}^{-2}$.

Finally, the enthalpy of solvation of an asphaltene molecule in liquid paraffin was calculated as a difference in the enthalpies of a single asphaltene in paraffin (140 *n*-eicosane chains) and in vacuum.

B. Atomistic simulations

Most atomistic simulation data were taken from our earlier work,¹⁹ where paraffin–asphaltene systems were studied with the use of two all-atom force fields, General AMBER Force Field (GAFF)⁶⁴ and CHARMM36.^{65,66} In particular, atomistic analogs of systems PAR-ASP-4, PAR-ASP-8, PAR-ASP-17, PAR-ASP-30, PAR-ASP-44, PAR-ASPM-4, PAR-ASPM-8, PAR-ASPM-17, PAR-ASPM-30, and PAR-ASPM-44 (see Table I) were studied in Ref. 19. Furthermore, several additional systems were considered in this paper for the sake of comparison with the outcome of mesoscale simulations. These include the PAR system (GAFF and CHARMM36 force fields), the PAR-ASPM-44 system with modified charge sets (GAFF and CHARMM36 force fields), and the compressed PAR-ASPM-44 system (the GAFF force field).

According to the original parameterization, the Lennard-Jones interactions were cut off at 0.9 nm (the GAFF force field)⁶⁴ and 1.2 nm (the CHARMM36 force field).^{65,66} The CHARMM36 force field also employs a function that smoothly switches the forces to zero between 1.0 and 1.2 nm.^{65,66} To handle electrostatic interactions, the particle-mesh Ewald method was employed.⁶⁷ The bonds between carbon and hydrogen atoms were constrained with the P-LINCS algorithm.⁶⁸ The systems were simulated in the NpT ensemble at $p = 1$ bar and $T = 450$ K, except for the compressed PAR-ASPM-44 system, where the NVT ensemble was employed. The temperature and pressure were controlled by the Nose–Hoover thermostat^{69,70} (with a time constant of 1 ps) and the

Parrinello–Rahman barostat⁵⁰ (with a time constant of 5 ps), respectively. The time step was set to 2 fs. Each additional system was simulated for 200 ns. The Gromacs suite (v. 2018.6) was used for all simulations.^{52,53}

In addition, we evaluated the free energy of dimerization of modified asphaltenes in liquid paraffin (the CHARMM36 force field). We used the umbrella sampling technique to calculate the PMF profile for two asphaltenes in the paraffin environment. The overall approach for calculating the PMF profile from atomistic simulations was the same as that employed for mesoscale simulations; see Sec. II A. The system consisted of two modified asphaltenes and 135 *n*-eicosane chains (8500 atoms in total). The distance between the centers of mass of the asphaltenes was varied from 0.3 to 2.0 nm with a step of 0.1 nm, resulting in 18 different configurations. Each window for umbrella sampling was simulated for 50 ns with a force constant of 1000 kJ mol⁻¹ nm⁻², and the last 30 ns of trajectories were used for computing the potential of the mean force. Furthermore, the asphaltene–asphaltene PMF in vacuum and the solvation enthalpy of an asphaltene in a paraffin environment were calculated in the same fashion as in Martini simulations.

III. RESULTS

A. Refining the force field: free energy of asphaltene dimerization

Initial test runs of paraffin–asphaltene systems revealed severe issues with the standard Martini force field. When modified asphaltenes without aliphatic side groups were considered, we observed irreversible aggregation of asphaltene molecules at the very beginning of simulations, which resulted in phase separation at large asphaltene concentrations. The translational mobility of asphaltenes in such aggregates turned out to be very limited; the normal diffusion of asphaltenes was not achieved on a microsecond time scale. Such behavior was not witnessed in atomistic simulations of the same systems as reported in our earlier study.¹⁹ Therefore, one can conclude that the standard Martini force field considerably overestimates the asphaltene–asphaltene interactions as compared to atomistic models.

To quantify this effect, we calculated the free energy of asphaltene dimerization from both coarse-grained and atomistic simulations. Since asphaltene aggregation is mainly governed by the π – π interactions between the asphaltene's aromatic cores, for such calculations we considered modified asphaltenes with aliphatic side chains cut off. Furthermore, it was shown that among the atomistic GAFF and CHARMM36 force fields used for computer simulations of asphaltenes of the same type, the latter gave stronger aggregation of asphaltenes.¹⁹ Therefore, we chose to compare the free energies of asphaltene dimerization of the standard coarse-grained Martini and atomistic CHARMM36 force fields; see Fig. 2.

As is evident from Fig. 2, both PMF profiles have minima at small distances between the two asphaltenes (binding of asphaltene aromatic cores) and become zero at large distances (no asphaltene interactions). For the atomistic CHARMM36 force field, the PMF minimum is located at 0.36 nm, and its depth (corresponding to the dimerization free energy) amounts to 11.1 kJ/mol. We note that the obtained aggregation energy agrees well with that reported in Ref. 30 for other types of asphaltenes and the GROMOS 54A7 force field. In turn, for the standard Martini force field, the PMF

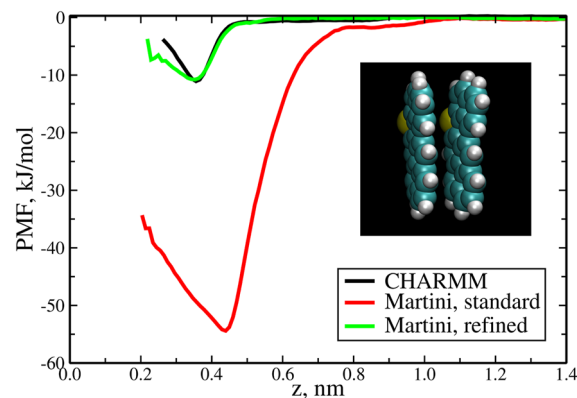


FIG. 2. Free energy profiles for the binding of two asphaltene molecules (asphaltene dimerization) in liquid paraffin as a function of the distance between the centers of mass of asphaltenes. Shown are the results for the atomistic CHARMM36 force field as well as for the standard and refined Martini force fields.

minimum is found farther away (at 0.44 nm), and the free energy of asphaltene dimerization equals 54.4 kJ/mol, which exceeds by 41.3 kJ/mol the free energy obtained from atomistic simulations. Therefore, the standard Martini force field indeed overestimates asphaltene dimerization.

To get insight into the source of such a discrepancy, we calculated the free energy of asphaltene dimerization in vacuum as well as the enthalpy of solvation of a single asphaltene in liquid paraffin. The free energy profiles in vacuum are very noisy; nevertheless, the free energy of asphaltene dimerization in vacuum can roughly be estimated as 161 ± 10 kJ/mol for the Martini model and 80 ± 10 kJ/mol for the CHARMM36 force field. The enthalpy of solvation of a single asphaltene in paraffin is found to be -4075 kJ/mol in Martini simulations, implying that the asphaltene–paraffin interactions are stronger than the interactions between paraffin molecules. In contrast, for the CHARMM36 force field, the enthalpy is large and positive (70 760 kJ/mol), which is a sign of strong interactions between paraffin molecules rather than between paraffin and asphaltenes. Therefore, we can conclude that the standard Martini model considerably overestimates both asphaltene–asphaltene and asphaltene–paraffin interactions. However, based on Fig. 2, interactions between asphaltene molecules are overestimated to a greater degree.

To make the Martini force field more realistic, we iteratively weakened the asphaltene–asphaltene (SC5–SC5) and asphaltene–paraffin (SC5–C1) interactions until the position of the PMF minimum, as well as the depth of the well, practically coincided for both coarse-grained and atomistic simulations. All in all, we performed around 30 iterations, and for each new set of Martini force field parameters, we recalculated the PMF profile of asphaltene dimerization.³⁰ Finally, we ended up with a CG parameter set that provides the best match with atomistic simulations: the dimerization free energy of 10.8 kJ/mol and the position of the PMF minimum at 0.36 nm; see Fig. 2. A new, refined set of Martini parameters is presented in Table SI. In the following, this parameter set will be employed for all coarse-grained simulations of paraffin–asphaltene systems.

B. Aggregation behavior of asphaltenes

In Fig. 3, we show typical snapshots of paraffin samples filled with native and modified asphaltenes of different concentrations. It is seen that asphaltenes with aliphatic side groups are distributed more evenly over paraffin samples as compared to their modified counterparts. This difference, which is more clearly seen in Figs. 3(b) and 3(e) for moderate concentrations of asphaltenes, originates from much weaker interactions between asphaltenes that have aliphatic periphery. It is also translated into the mass density of paraffin–asphaltene samples; see Fig. 4. For unfilled paraffin ($C_{\text{asph}} = 0$), the mass density of the Martini system exceeds the densities of both the atomistic CHARMM36 and GAFF samples. Therefore, the Martini coarse-grained force field follows the same trend as united-atom models, in which a CH_2 group is treated as a single interaction site. Our previous computational study showed that the united-atom models generally led to higher densities of liquid *n*-eicosane as compared to their all-atom counterparts.^{58,59} It is also noteworthy that our earlier atomistic study of the same systems¹⁹ gave us an opportunity to compare the outcome of mesoscale simulations with that of atomistic simulations performed with two different force fields. This is important because, in this way, we can emphasize the fact that the results of atomistic simulations can vary considerably depending on the model. In particular, the difference in the *n*-eicosane density of Martini and CHARMM36 samples is very close to that observed for atomistic CHARMM36 and GAFF models; see Fig. 4.

As for the mass densities of paraffin–asphaltene systems, we observe somewhat different trends for native and modified

asphaltenes. The density of paraffin samples grows almost linearly with the concentration of modified asphaltenes without aliphatic chains; see Fig. 4(b). This implies that most modified asphaltenes are incorporated into aggregates whose density is higher than the density of paraffin; the larger the fraction of the aggregates, the higher the density. In turn, the density plots $\rho(C_{\text{asph}})$ for native asphaltenes deviate from the linear dependence; see Fig. 4(a). The reason for that is twofold. First, native asphaltenes mix much better with paraffin due to their aliphatic side chains, so there is a fraction of asphaltenes that do not aggregate. And second, part of the native asphaltene molecules (the aliphatic periphery) has the same density as paraffin.

To quantify the asphaltene aggregation, we carried out a cluster analysis of asphaltene molecules with the use of the Gromacs routine `gmx clustsize`.⁵² For the sake of comparison with atomistic simulations, the analysis was performed according to the protocol developed in our earlier studies.^{19,28} For both native and modified asphaltenes, the cluster analysis was applied only to the asphaltene's aromatic cores.³³ Two asphaltene molecules were treated as being in the same aggregate if the smallest distance between the core beads of the asphaltenes did not exceed a cutoff radius of 0.45 nm. Once asphaltene molecules were assigned to aggregates, we computed the average number of asphaltenes per aggregate (the aggregate size) and the average number of aggregates in the system.

In Fig. 5, we present both these characteristics for paraffin samples filled with native asphaltenes. It is seen that CG asphaltenes follow the same pattern as their atomistic counterparts: one has a slow increase in aggregate size with asphaltene concentration;

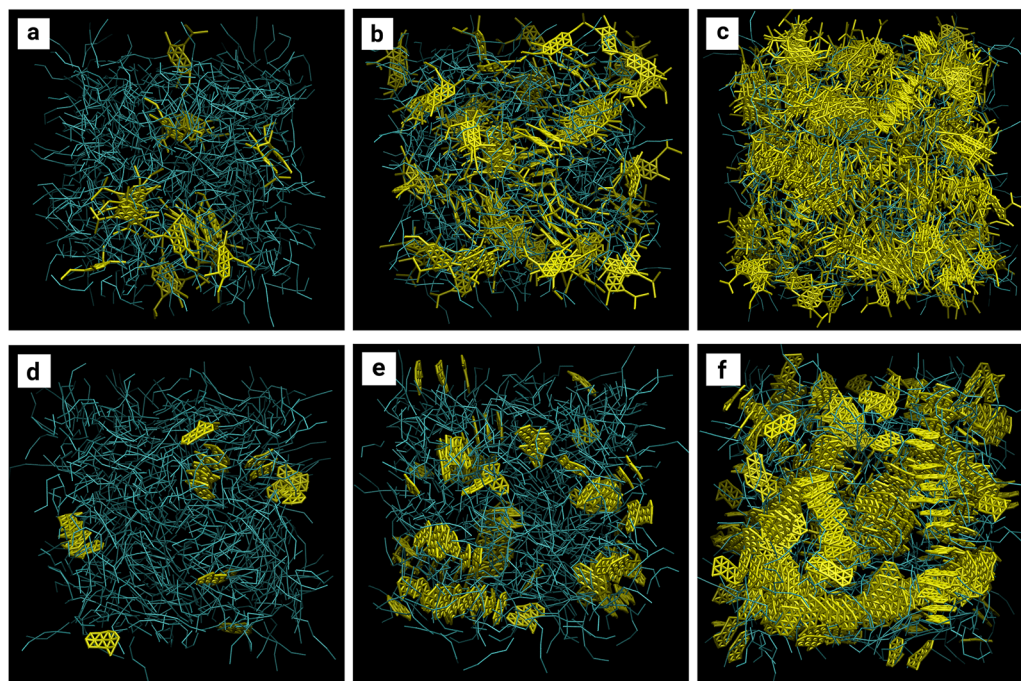


FIG. 3. Representative snapshots of paraffin samples filled with native [(a), (b), and (c)] and modified [(d), (e), and (f)] asphaltenes. Shown are the snapshots for asphaltene concentrations of 4 [(a) and (d)], 17 [(b) and (e)], and 44 [(c) and (f)] mol %. ASP and ASPM are shown in yellow; paraffin chains are shown in cyan.

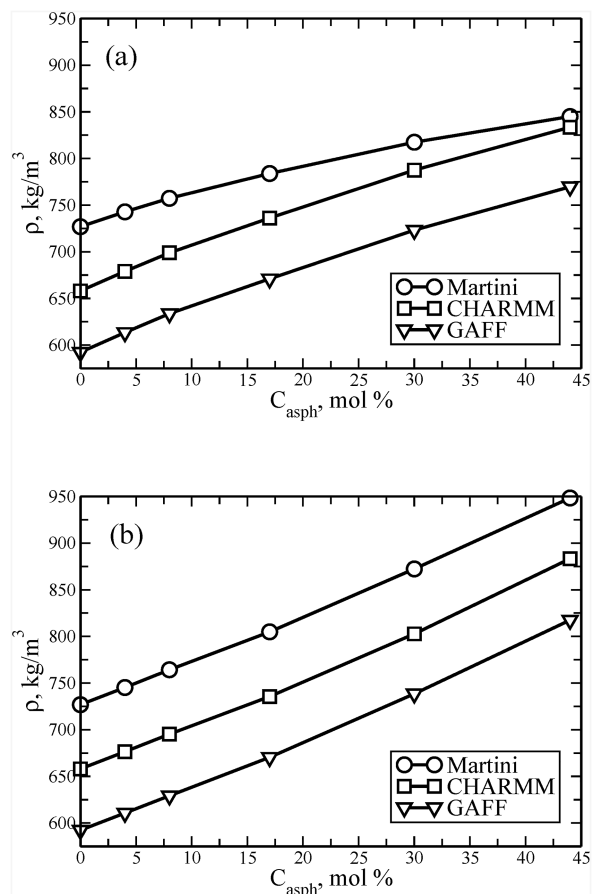


FIG. 4. Mass density of paraffin–asphaltene systems as a function of the concentration of native (a) and modified (b) asphaltenes. Shown are the results for the coarse-grained Martini force field as well as for the atomistic CHARMM36 and GAFF models.

see Fig. 5(a). On average, the CG aggregates are larger than those in the CHARMM36 and GAFF simulations, which implies that the coarse-graining of aliphatic side chains reduces their steric constraints, thereby promoting the asphaltene's aggregation. However, the absolute values of the average aggregate size remain relatively small after coarse-graining, so the Martini force field provides a reasonable description of the aggregation of asphaltenes with peripheral aliphatic groups. The same applies to the average number of aggregates, which increases linearly with asphaltene concentration, although mesoscale simulations give a flatter dependence compared to atomistic ones; see Fig. 5(b).

When it comes to asphaltene molecules with aliphatic side groups cut off, the situation becomes more involved. Two aspects are to be noticed from the concentration dependence of the aggregate size in Fig. 6(a): (i) for moderate asphaltene concentrations (up to 30 mol %), the aggregate size in CG simulations practically coincides with that in GAFF (but not in CHARMM36) simulations, and (ii) the average size of aggregates in CG simulations becomes abnormally large at the highest asphaltene concentration of 44 mol %.

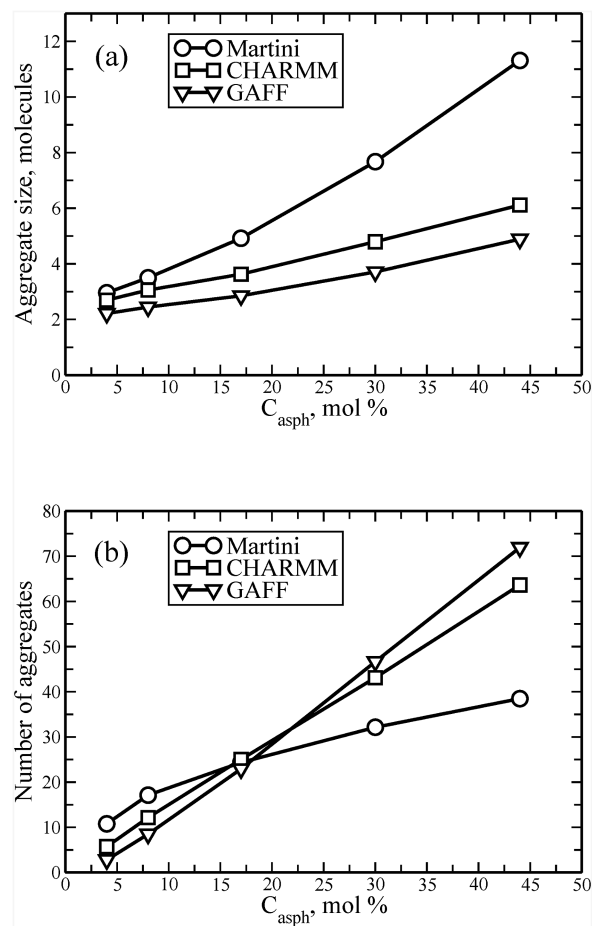


FIG. 5. The average number of asphaltenes per aggregate (a) and the average number of aggregates (b) as a function of the concentration of native asphaltenes (ASP) in the system. Shown are the results for the coarse-grained Martini force field as well as the atomistic CHARMM36 and GAFF force fields.

We recall that the CHARMM36 force field was used for refining the Martini model; therefore, it is rather surprising that the aggregation behavior in Martini simulations is much closer to what is observed in GAFF simulations. In simple terms, this implies that fitting the dimerization energy is not enough to capture the aggregation behavior observed in CHARMM36 simulations. The dimerization is responsible for the formation of extended stacks of asphaltenes. However, in CHARMM36 simulations, one can also witness the interactions of different stacks with each other, resulting in the formation of an ordered columnar super-aggregate.¹⁹ The possible nature of such “stack–stack” interactions is electrostatics. However, since the CG asphaltene model developed in this work does not include any partial charges, we do not account for these interactions in our CG model.

Whether to include charges in the CG model of asphaltenes is not a simple question, although some related studies chose to do so.³⁰ Here, having at hand the results of atomistic simulations performed with two different force fields (CHARMM36 and GAFF)

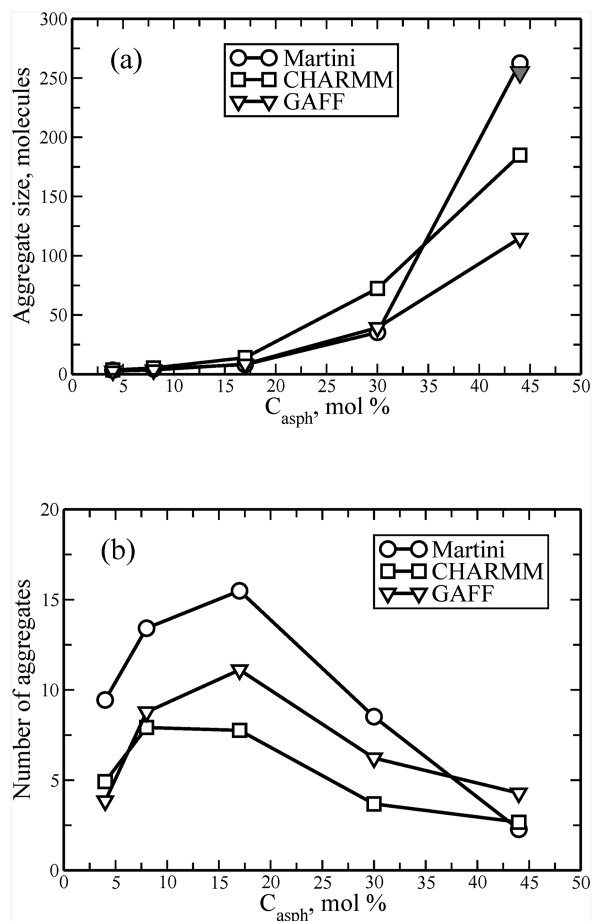


FIG. 6. The average number of asphaltenes per aggregate (a) and the average number of aggregates (b) as a function of the concentration of modified asphaltenes (ASPM) in the system. Shown are the results for the coarse-grained Martini force field as well as the atomistic CHARMM36 and GAFF force fields. The filled triangle corresponds to the compressed PAR-ASPM-44 system (the GAFF force field).

allows us to get the bigger picture. The atomistic GAFF force field does include the partial charges; however, the charges themselves cannot ensure that a columnar super-aggregate is formed, in contrast to the CHARMM36 force field.¹⁹ This could indicate that strong “stack–stack” interactions are most likely a specific feature of the CHARMM36 force field. Indeed, replacing the GAFF partial charges with the CHARMM36 charges in GAFF simulations of the PAR-ASPM-44 system does lead to the formation of a columnar super-aggregate; see Fig. S2. Vice versa, incorporating GAFF partial charges into CHARMM36 simulations destroys the columnar super-aggregate in the PAR-ASPM-44 system (data not shown). Due to the lack of direct comparison with experimental data, it is hard to judge which atomistic force field provides a better description. Therefore, we can conclude that our CG model performs reasonably well at moderate asphaltene concentrations as it agrees with at least one of the atomistic models; see Fig. 6(a).

As for the abnormally large size of CG aggregates at $C_{\text{asph}} = 44$ mol. %, this could be due to the larger density of CG systems as compared to atomistic ones; see Fig. 4(b). As was discussed above, the extended asphaltene stacks in CG simulations do not form regular columnar super-aggregates. However, they can partly overlap when the system density increases (or the free volume drops), so most asphaltene molecules belong to a large disordered aggregate; see Fig. 3(f). To test this hypothesis, we compressed the GAFF sample of the PAR-ASPM-44 system to a state where the mass density of both the Martini and GAFF systems was the same. The cluster analysis performed for the compressed GAFF sample showed that its average aggregate size, indeed, became very close to that of the Martini sample [see Fig. 6(a)], confirming the key role of the system density.

It is also important to note that the average size of asphaltene aggregates can be considered an indirect measure of cluster stability. At high asphaltene concentrations, very large clusters can also be formed in the CHARMM36 and GAFF simulations. To illustrate this, in Fig. S3, we present the average number of modified asphaltenes in the largest aggregate. It is seen that at $C_{\text{asph}} = 44$ mol. %, the sizes of the largest clusters almost coincide in the Martini, CHARMM36, and GAFF simulations. However, the asphaltene clusters are considerably less stable in atomistic simulations compared to the situation when a coarse-grained model is employed, leading to a smaller average size of aggregates; see Fig. 6(a).

Another interesting feature of the aggregation of modified asphaltenes is the non-monotonic concentration dependence of the number of aggregates; see Fig. 6(b). When asphaltene concentration is low, asphaltene molecules prefer to form relatively small clusters, so the number of clusters increases with concentration. However, at higher concentrations ($C_{\text{asph}} > 17$ mol. %), these small clusters start to merge into larger aggregates, and the number of aggregates drops with asphaltene concentration. As is obvious from Fig. 6(b), our CG model for asphaltene aggregation successfully reproduces such a non-monotonic behavior.

A more detailed insight into the changes in the aggregation behavior of modified asphaltenes with concentration can be gained from the distribution of cluster sizes; see Fig. S4. At asphaltene concentrations of 17 mol. % (and smaller), one has the formation of finite clusters of relatively small sizes. At a concentration of 30 mol. %, the distribution of cluster sizes becomes bimodal: in addition to the peak corresponding to small clusters, a second peak develops. This peak is located in the domain of large aggregate sizes and indicates a tendency of the system to phase separation. However, this separation does not occur: there are still a considerable number of clusters of intermediate sizes (between the two peaks), implying that the formation of large clusters is a reversible process. Note that the overall picture resembles results reported in earlier coarse-grained simulations of asphaltenes in *n*-heptane.³³ At the maximal asphaltene concentration (44 mol. %), the distribution remains bimodal, but all the intermediate states between the two peaks disappear; see Fig. S4. In fact, we witness a situation when only very small clusters of asphaltenes (up to 15 molecules) can be found in the paraffin phase. Once their aggregate size exceeds this threshold, the small cluster becomes part of a large asphaltene super-aggregate. Such a behavior is a signature of phase separation.

Although the thermal conductivity of paraffin–asphaltene composites is beyond the scope of the present study, it is important to qualitatively link the asphaltenes' aggregation behavior with the thermally conductive properties of the systems at hand. As shown above, removing aliphatic side groups from asphaltenes promotes the formation of ordered stacks of asphaltene molecules. Such asphaltene aggregates could serve as thermal conduction paths, thereby accelerating heat transfer. Therefore, we can expect that chemical modification of asphaltenes dispersed in paraffin enhances the thermal conductivity of the composites. This was, indeed, observed in atomistic computer simulations of paraffin–asphaltene systems.¹⁹

Another important aspect to consider is the polydispersity of asphaltene molecules, which makes computer modeling of such systems very challenging.^{25,27} In our study, we chose a typical representative of petroleum asphaltenes as predicted by experiments: a single small polyaromatic core decorated with aliphatic groups.¹ As we have shown, such native asphaltenes form reactively small clusters due to steric restraints imposed by the aliphatic periphery; see Fig. 5. Therefore, one can expect that a polydisperse asphaltene system exhibits a similar behavior, provided that the asphaltenes' aromatic cores are still relatively small and the sufficiently massive aliphatic groups are present in asphaltenes. When the aliphatic periphery is very small or completely cut off, as in our case, the situation becomes less certain. However, one could speculate that the presence of polycyclic hydrocarbon molecules with aromatic cores of various sizes could stabilize asphaltene aggregates, as such molecules could more effectively fill the defects in the aggregates.

C. Diffusion properties

The asphaltene's aggregation behavior can also be characterized by the translational mobility of asphaltene molecules in liquid paraffin. As mentioned in Sec. III A, the standard Martini force field considerably overestimated the asphaltene aggregation, leading to a very low mobility of asphaltenes. The refined Martini model shows a much more realistic behavior: the aggregation of asphaltenes is not irreversible anymore, and the normal diffusion is already easily achieved after tens of nanoseconds. This allowed us to compute the diffusion coefficients from the mean-squared displacement curves; the results for paraffin systems filled with both native and modified asphaltenes are presented in Fig. 7.

Remarkably, the diffusion coefficients of CG asphaltenes show very good agreement with those obtained from CHARMM36 simulations. We recall that the dimerization energy of CG asphaltenes was fitted to the CHARMM36 data. Therefore, one can conclude that the lateral mobility of asphaltenes is mostly governed by asphaltene dimerization rather than interactions between asphaltene stacks. Interestingly, the diffusion coefficients of modified asphaltenes are systematically larger than those measured for native asphaltenes with aliphatic side groups (by ~ 2 to 2.5 times); see Fig. 7. This finding seems counterintuitive since modified asphaltenes form much larger aggregates than native asphaltenes do; see Figs. 5 and 6. As mentioned above, the native asphaltenes are embedded in the paraffin environment to a greater extent compared to their modified counterparts because the aliphatic side groups of the native asphaltenes are able to mix (and interact) with paraffin chains. This factor seems

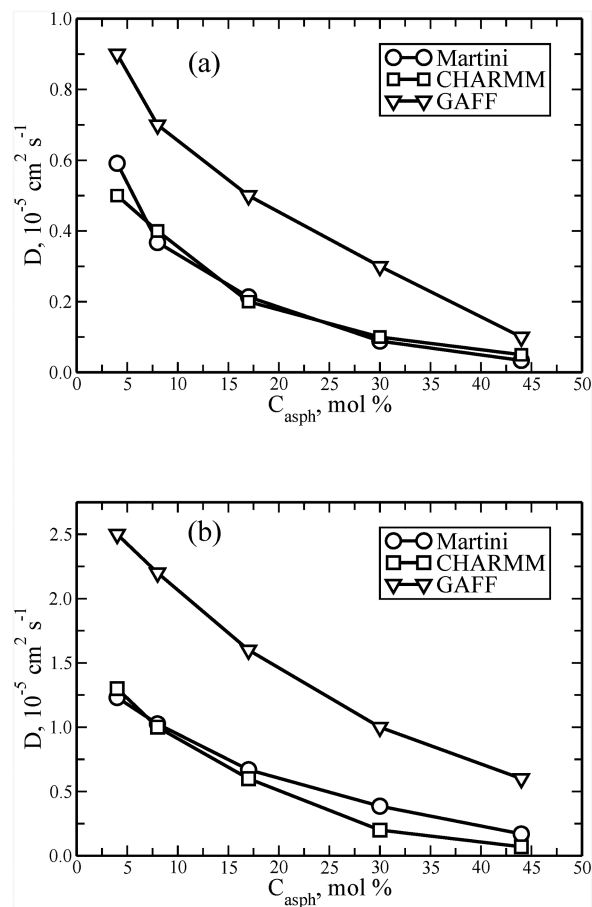


FIG. 7. Diffusion coefficients of asphaltene molecules as a function of the concentration of native (a) and modified (b) asphaltenes. Shown are the results for the coarse-grained Martini force field as well as for the atomistic CHARMM36 and GAFF models.

to have a larger impact on the lateral mobility of asphaltenes as compared to the ability of asphaltenes to aggregate.

Besides asphaltenes, we also considered the lateral mobility of paraffin chains in paraffin–asphaltene systems at hand; see Fig. 8. It is seen that the concentration dependence of diffusion coefficients of CG paraffin chains is in between the corresponding curves obtained from CHARMM36 and GAFF simulations, indicating a reasonable agreement between mesoscale and atomistic simulations. Adding asphaltenes to the paraffin matrix slows down the mobility of paraffin chains; this effect is more pronounced for high asphaltene concentrations as well as for native asphaltenes with aliphatic side groups; see Fig. 8. However, there is a noticeable exception: when a small fraction of modified CG asphaltenes (4 mol.%) is introduced into paraffin, the diffusion coefficient of paraffin chains slightly increases; see Fig. 8(b). We attribute this unusual effect to the small size of the simulation box. Indeed, if a simulation box in CG simulations of unfilled paraffin is too small, this could lead to the artificial cutting off of long-range hydrodynamic interactions and correspondingly reduce the diffusion coefficient of paraffin

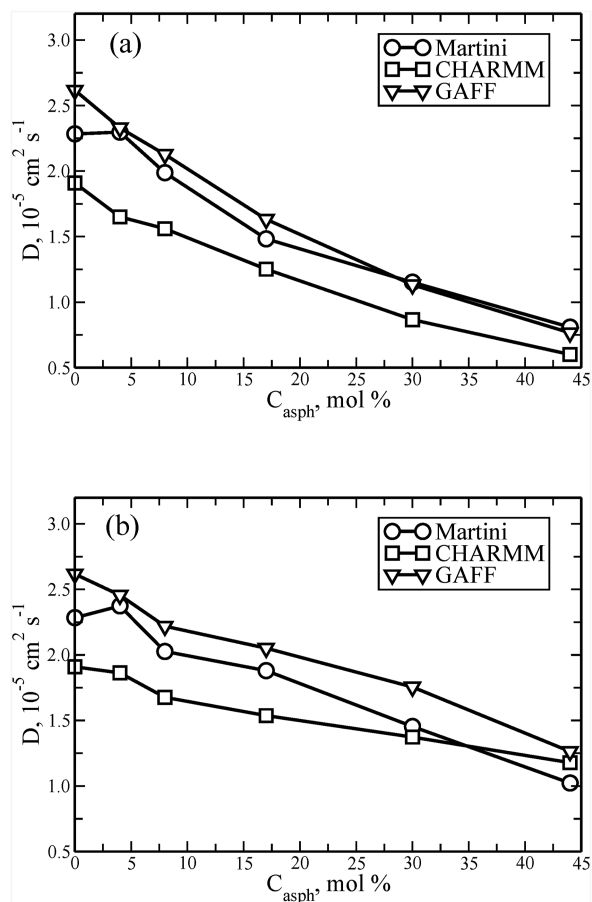


FIG. 8. Diffusion coefficients of paraffin molecules as a function of the concentration of native (a) and modified (b) asphaltenes. Shown are the results for the coarse-grained Martini force field as well as for the atomistic CHARMM36 and GAFF models.

chains.^{71,72} Adding a small fraction of asphaltenes to paraffin screens the hydrodynamic interactions and increases the diffusion coefficient. Note that this holds only for a very small concentration of asphaltenes (4 mol. %) because asphaltene molecules themselves are able to slow down the mobility of paraffin chains.

To conclude this section, it is worth discussing how the time scales of atomistic and coarse-grained models are related. In general, coarse-graining makes the energy landscape smoother, which could potentially enhance the sampling of energy states and speed up dynamics. In coarse-grained Martini simulations, one often applies a speed-up factor of 4 when comparing self-diffusion with the outcome of atomistic simulations.⁴⁶ However, this speed-up factor is not universal and is system-specific. In particular, for alkanes, a speed-up is known to be small (if present at all).⁴⁸ This is exactly what we observed for paraffin (*n*-eicosane) in our system; see Fig. 8. Furthermore, a comparison of the diffusion coefficients of asphaltenes in Martini and CHARMM simulations also indicates that coarse-graining does not speed up the dynamics of asphaltene molecules (Fig. 7).

D. Large systems

As demonstrated in Secs. III B and III C, our refined coarse-grained model for asphaltene aggregation performed reasonably well when compared to the outcome of atomistic simulations. Now, we can use the advantages of the coarse-grained Martini force field and consider significantly larger systems. To this end, we increased the number of molecules in paraffin–asphaltene systems by a factor of 10 and performed simulations of the large systems on a microsecond time scale. In particular, the largest system at hand comprises almost 4000 asphaltene molecules; see Table I.

In Fig. 9, we present the average size of asphaltene aggregates for both standard and large systems. For native asphaltenes, we do not witness any size effects in the asphaltene's aggregation behavior; the asphaltene clusters remain relatively small. For modified asphaltenes without aliphatic side groups, this also holds for moderate asphaltene concentrations up to 30 mol. %. An obvious exclusion is the PAR-ASPM-44-Large system. As mentioned above, at such a large concentration, different stacks of modified asphaltenes overlap with a formation of big, disordered aggregates; see Figs. 3(f) and 6(a). Furthermore, the cluster size distribution suggests that the system is separated into two phases; see Fig. S4. Therefore, it is not surprising that the asphaltene super-aggregates (the asphaltene phase) grow when the size of the system increases, as is clearly shown in Fig. 9. Remarkably, the distribution of cluster sizes for the PAR-ASPM-44-Large system follows the same pattern as the system of smaller size (Fig. S4): there are two peaks corresponding to small and very large aggregates with no intermediate states (data not shown). What is more, the ratio of the asphaltenes in super-aggregates to the asphaltenes dispersed in paraffin amounts to ~ 98 and remains unchanged with the size of the system.

As for the diffusion properties of paraffin–asphaltene systems, the system size slightly increases the translational mobility of asphaltene molecules; see Fig. 10(a). This effect almost vanishes at high asphaltene concentrations, while it can be more pronounced in systems with low contents of modified asphaltenes. Accordingly, the largest increase in the diffusion coefficient (around 25%) is observed

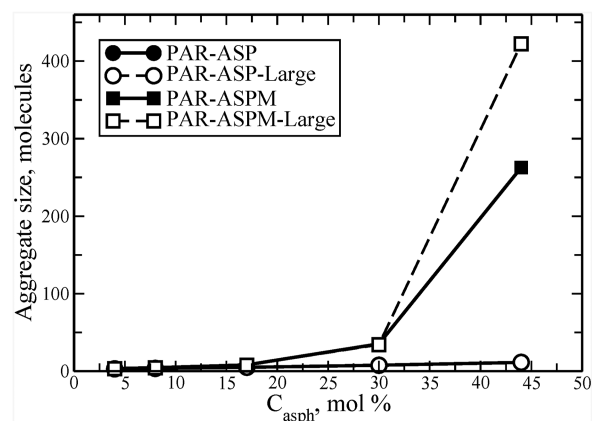


FIG. 9. The average number of asphaltenes per aggregate as a function of asphaltene concentration. Shown are the results for the CG systems of standard and large sizes.

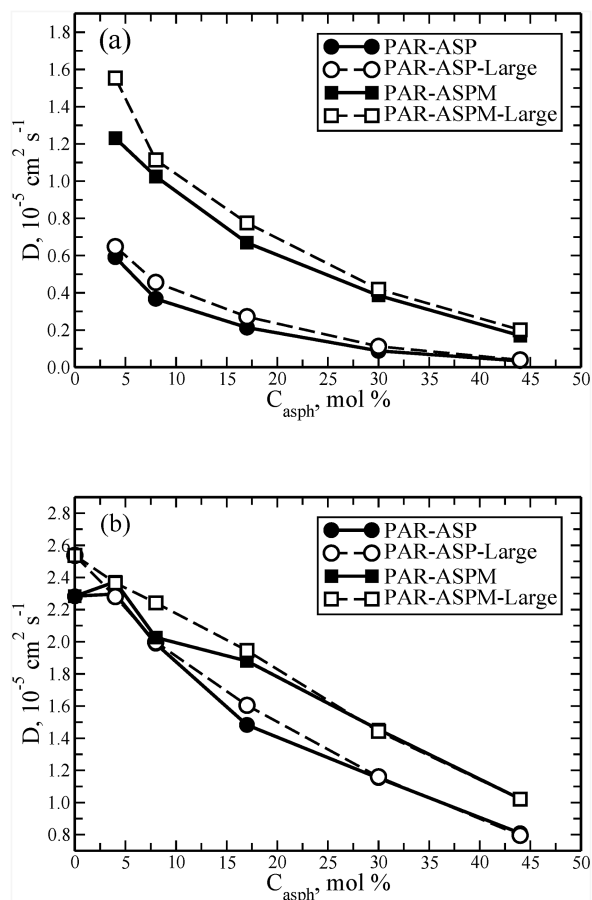


FIG. 10. Diffusion coefficients of asphaltenes (a) and paraffin chains (b) as a function of asphaltene concentration. Shown are the results for the CG systems of standard and large sizes.

for the PAR-ASPM-4-Large system; see Fig. 10(a). As in smaller systems, the mobility of modified asphaltenes is systematically higher than that of native molecules whose aliphatic side groups mix with paraffin chains.

In turn, the concentration dependences of the diffusion coefficients of paraffin chains become smoother when the system size increases; see Fig. 10(b). It is noteworthy that the abnormal increase in the diffusion coefficient of paraffin chains at small asphaltene concentrations disappears in the case of large systems. As mentioned in Sec. III D, this abnormal behavior was due to size effects. Therefore, increasing the number of molecules in the system considerably weakened the artifacts associated with the finite size of a simulation box. In particular, we observe a noticeable increase in the diffusion coefficient of *n*-eicosane chains in unfilled paraffin samples when the system size becomes larger: $\Delta D = 0.26 \times 10^{-5} \text{ cm}^2/\text{s}$ when the length of a cubic simulation box L increases from 6.9 nm (the PAR system) to 14.7 nm (the PAR-Large system). It is interesting to compare this computational result with theoretical predictions for diffusion coefficients in simulations under periodic boundary conditions.⁷³ According to Ref. 73, the diffusion coefficient D_{PBC} measured in

a system of finite size should be corrected as follows: $D_0 = D_{\text{PBC}} + 2.837297 k_B T / (6\pi\eta L)$, where η is the shear viscosity of the solvent. Following the procedure outlined in our previous paper,⁵⁸ the shear viscosity of liquid *n*-eicosane in the framework of the Martini model was estimated to be 0.5 m Pa s, which is rather close to the experimental value of 0.594 m Pa s; see Ref. 74. It is noteworthy that the computed value of the shear viscosity turned out to be insensitive to the system size. Correspondingly, substituting the values of η and L into the equation, we obtain $\Delta D = 0.15 \times 10^{-5} \text{ cm}^2/\text{s}$. Therefore, the theoretical prediction for the increase in the diffusion coefficient of liquid paraffin agrees reasonably well with the outcome of mesoscale computer simulations ($0.26 \times 10^{-5} \text{ cm}^2/\text{s}$).

IV. CONCLUSIONS

Asphaltenes are abundant and non-expensive aromatic side products of the deep refining of crude oil. Asphaltene molecules represent a new promising class of carbon nanofillers that could be used in polymer nanocomposites, solar cells, domestic heat storage devices, etc. As the polycyclic aromatic core of asphaltenes is normally decorated with aliphatic side groups, the aggregation behavior of asphaltenes can be considerably enhanced through an appropriate chemical modification that minimizes the aliphatic fraction of asphaltenes. Besides numerous experimental studies in the field, asphaltenes have recently attracted attention from several computational research groups.

In this work, we developed a realistic coarse-grained model for studying the aggregation behavior of asphaltenes in liquid paraffin. This type of system is of particular interest from the point of view of heat storage devices based on organic phase-change materials. Both native asphaltenes and chemically modified asphaltenes with aliphatic side groups cut off were considered. Our coarse-grained model was based on the Martini force field. To refine the model, the free energy of asphaltene dimerization was adjusted to the outcome of atomistic simulations. The resulting coarse-grained description of asphaltene molecules allowed us to reproduce the aggregation behavior and diffusion properties of asphaltenes, which were observed in computer simulations performed with high-resolution models. Importantly, the results of mesoscale simulations were compared to the outcome of simulations carried out with two different full-atom force fields (CHARMM36 and GAFF). This allowed us to verify our coarse-grained model and also to better understand the differences between various atomistic models.

With the realistic coarse-grained model at hand, we explored for the first time the aggregation of thousands of asphaltene molecules in liquid paraffin on a microsecond time scale. We showed that native asphaltenes with aliphatic side groups were distributed rather evenly over the system at all considered asphaltene concentrations. Their aggregation behavior was found to be insensitive to the size of a simulation box. In the case of modified asphaltenes without aliphatic periphery, we observed the formation of extended stacks of asphaltenes. When the asphaltene concentration becomes very large (44 mol %), these stacks partly overlap, leading to the formation of large, disordered super-aggregates and correspondingly to phase separation. Because of the phase separation, the size of the super-aggregates depends on the system size. In turn, diffusion coefficients of asphaltenes were found to be not very sensitive to the size of a simulation box: enlarging the system leads to some increase in

the diffusion coefficient; this effect vanishes at high asphaltene concentrations. The mobility of modified asphaltenes is systematically higher than that of their native counterparts because the aliphatic periphery of native asphaltenes mixes with paraffin chains, slowing down the asphaltene diffusion.

Overall, our computational findings highlight the possible inherent limitations of computer modeling when it comes to studying asphaltene aggregation in liquid paraffin. In particular, we show that the asphaltene aggregate size measured in simulations should be taken with caution, as it can depend on the system size when the system undergoes a phase transition. It is also noteworthy that most computational findings for the aggregation of modified asphaltene molecules without aliphatic periphery can be transferred to the aggregation behavior of polycyclic aromatic hydrocarbons, such as coronene, ovalene, and hexabenzocoronene.

SUPPLEMENTARY MATERIAL

See the supplementary material for more information about the parameters of the coarse-grained force field, cooling-rate simulations of paraffin samples, atomistic simulations of paraffin–asphaltene systems, and the cluster analysis.

ACKNOWLEDGMENTS

This work was supported by the Russian Science Foundation under Agreement No. 19-13-00178 (A.A.G. and V.M.N.). The simulations were performed using the computational resources of the Institute of Macromolecular Compounds RAS, the resources of the Federal collective usage center “Complex for Simulation and Data Processing for Mega-science Facilities” at the NRC “Kurchatov Institute” (<http://ckp.nrcki.ru/>), and the equipment of the shared research facilities of HPC computing resources at the Lomonosov Moscow State University.

AUTHOR DECLARATIONS

Conflict of Interest

The authors have no conflicts to disclose.

Author Contributions

The manuscript was written through contribution of all authors. All authors have given approval of the final version of the manuscript.

Andrey A. Gurtovenko: Conceptualization (equal); Data curation (equal); Funding acquisition (equal); Investigation (equal); Methodology (equal); Project administration (equal); Visualization (equal); Writing – original draft (equal); Writing – review & editing (equal). **Victor M. Nazarychev:** Investigation (equal); Methodology (equal); Visualization (equal); Writing – review & editing (equal). **Artem D. Glova:** Investigation (equal); Methodology (equal); Visualization (equal); Writing – review & editing (equal). **Sergey V. Larin:** Conceptualization (equal); Investigation (equal); Writing – review &

editing (equal). **Sergey V. Lyulin:** Conceptualization (equal); Investigation (equal); Writing – review & editing (equal).

DATA AVAILABILITY

The data that support the findings of this study are available from the corresponding author upon reasonable request.

REFERENCES

- O. C. Mullins, *Annu. Rev. Anal. Chem.* **4**, 393 (2011).
- J. S. Buckley, *Energy Fuels* **26**, 4086 (2012).
- M. P. Hoepfner, V. Limsakoune, V. Chuenmeechao, T. Maqbool, and H. S. Fogler, *Energy Fuels* **27**, 725 (2013).
- J. J. Adams, *Energy Fuels* **28**, 2831 (2014).
- S. Fakher, M. Ahdaya, M. Elturki, and A. Imqam, *J. Pet. Explor. Prod. Technol.* **10**, 1183 (2020).
- S. N. Gorbacheva, Y. Y. Borisova, V. V. Makarova, S. V. Antonov, D. N. Borisov, and M. R. Yakubov, *Molecules* **28**, 949 (2023).
- Asphaltenes, Heavy Oils and Petroleomics*, edited by O. C. Mullins, E. Y. Sheu, A. Hammami, and A. G. Marshall (Springer, New York, 2007).
- K. Akbarzadeh, A. Hammami, A. Kharrat, D. Zhang, S. Allenson, J. Creek, S. Kabir, A. Jamaluddin, A. Marshall, R. Rodgers, O. Mullins, and T. Solbakken, *Oil F. Rev.* **19**, 22 (2007).
- C. Vilas Bôas Fávero, T. Maqbool, M. Hoepfner, N. Haji-Akbari, and H. S. Fogler, *Adv. Colloid Interface Sci.* **244**, 267 (2017).
- H. Wu and M. R. Kessler, *RSC Adv.* **5**, 24264 (2015).
- H. Wu, V. K. Thakur, and M. R. Kessler, *J. Mater. Sci.* **51**, 2394 (2016).
- V. Y. Ignatenko, A. V. Kostyuk, J. V. Kostina, D. S. Bakhtin, V. V. Makarova, S. V. Antonov, and S. O. Ilyin, *Polym. Eng. Sci.* **60**, 1530 (2020).
- R. E. Abujnah, H. Sharif, B. Torres, K. Castillo, V. Gupta, and R. R. Chianelli, *J. Environ. Anal. Toxicol.* **6**, 345 (2016).
- V. V. Makarova, S. N. Gorbacheva, A. V. Kostyuk, S. V. Antonov, Y. Y. Borisova, D. N. Borisov, and M. R. Yakubov, *J. Energy Storage* **47**, 103595 (2022).
- S. V. Larin, V. V. Makarova, S. N. Gorbacheva, M. R. Yakubov, S. V. Antonov, N. I. Borzdun, A. D. Glova, V. M. Nazarychev, A. A. Gurtovenko, and S. V. Lyulin, *J. Chem. Phys.* **157**, 194702 (2022).
- M. N. Siddiqui and I. W. Kazi, *Pet. Sci. Technol.* **32**, 2987 (2014).
- H. M. S. Lababidi, H. M. Sabti, and F. S. AlHumaidan, *Fuel* **117**, 59 (2014).
- D. N. Borisov, L. E. Foss, K. V. Shabalin, L. I. Musin, and R. Z. Musin, *Chem. Technol. Fuels Oils* **55**, 552 (2019).
- A. D. Glova, V. M. Nazarychev, S. V. Larin, A. V. Lyulin, S. V. Lyulin, and A. A. Gurtovenko, *J. Mol. Liq.* **346**, 117112 (2022).
- X. Feng, V. Marcon, W. Pisula, M. R. Hansen, J. Kirkpatrick, F. Grozema, D. Andrienko, K. Kremer, and K. Müllen, *Nat. Mater.* **8**, 421 (2009).
- T. Wöhrle, I. Wurzbach, J. Kirres, A. Kostidou, N. Kapernaum, J. Litterscheidt, J. C. Haenle, P. Staffeld, A. Baro, F. Giesselmann, and S. Laschat, *Chem. Rev.* **116**, 1139 (2016).
- S. V. Lyulin, A. D. Glova, S. G. Falkovich, V. A. Ivanov, V. M. Nazarychev, A. V. Lyulin, S. V. Larin, S. V. Antonov, P. Ganan, and J. M. Kenny, *Pet. Chem.* **58**, 983 (2018).
- M. Sedghi, L. Goual, W. Welch, and J. Kubelka, *J. Phys. Chem. B* **117**, 5765 (2013).
- Y. Mikami, Y. Liang, T. Matsuoka, and E. S. Boek, *Energy Fuels* **27**, 1838 (2013).
- T. F. Headen, E. S. Boek, G. Jackson, T. S. Totton, and E. A. Müller, *Energy Fuels* **31**, 1108 (2017).
- S. Yaseen and G. A. Mansoori, *J. Pet. Sci. Eng.* **156**, 118 (2017).
- G. Javanbakht, M. Sedghi, W. R. W. Welch, L. Goual, and M. P. Hoepfner, *J. Mol. Liq.* **256**, 382 (2018).
- A. D. Glova, S. V. Larin, V. M. Nazarychev, J. M. Kenny, A. V. Lyulin, and S. V. Lyulin, *ACS Omega* **4**, 20005 (2019).
- B. Aguilera-Mercado, C. Herdes, J. Murgich, and E. A. Müller, *Energy Fuels* **20**, 327 (2006).

- ³⁰J. Wang and A. L. Ferguson, *J. Phys. Chem. B* **120**, 8016 (2016).
- ³¹S. H. Kim, K. D. Kim, H. Lee, and Y. K. Lee, *Chem. Eng. J.* **314**, 1 (2017).
- ³²J. Wang, M. Gayatri, and A. L. Ferguson, *J. Phys. Chem. B* **122**, 6627 (2018).
- ³³G. Jiménez-Serratos, T. S. Totton, G. Jackson, and E. A. Müller, *J. Phys. Chem. B* **123**, 2380 (2019).
- ³⁴J. Wong-Ekkabut, S. Baoukina, W. Triampo, I.-M. Tang, D. P. Tieleman, and L. Monticelli, *Nat. Nanotechnol.* **3**, 363 (2008).
- ³⁵E. J. Wallace and M. S. P. Sansom, *Nano Lett.* **7**, 1923 (2007).
- ³⁶N. Patra and P. Král, *J. Am. Chem. Soc.* **133**, 6146 (2011).
- ³⁷A. V. Titov, P. Král, and R. Pearson, *ACS Nano* **4**, 229 (2010).
- ³⁸N. Willems, A. Urtizberea, A. F. Verre, M. Iliut, M. Lelimosin, M. Hirtz, A. Vijayaraghavan, and M. S. P. Sansom, *ACS Nano* **11**, 1613 (2017).
- ³⁹G. Li, M. Han, Y. Tan, A. Meng, J. Li, and S. Li, *Constr. Build. Mater.* **263**, 120933 (2020).
- ⁴⁰R. Baron, D. Trzesniak, A. H. de Vries, A. Elsener, S. J. Marrink, and W. F. van Gunsteren, *ChemPhysChem* **8**, 452 (2007).
- ⁴¹R. Baron, A. H. de Vries, P. H. Hünenberger, and W. F. van Gunsteren, *J. Phys. Chem. B* **110**, 8464 (2006).
- ⁴²D. D. Li and M. L. Greenfield, *Fuel* **115**, 347 (2014).
- ⁴³M. B. Singh, N. Rampal, and A. Malani, *Energy Fuels* **32**, 8259 (2018).
- ⁴⁴Z. Dong, Z. Liu, P. Wang, and X. Gong, *Fuel* **189**, 155 (2017).
- ⁴⁵M. Xu, J. Yi, P. Qi, H. Wang, M. Marasteanu, and D. Feng, *Energy Fuels* **33**, 3187 (2019).
- ⁴⁶S. J. Marrink, H. J. Risselada, S. Yefimov, D. P. Tieleman, and A. H. de Vries, *J. Phys. Chem. B* **111**, 7812 (2007).
- ⁴⁷L. Monticelli, S. K. Kandasamy, X. Periole, R. G. Larson, D. P. Tieleman, and S.-J. Marrink, *J. Chem. Theory Comput.* **4**, 819 (2008).
- ⁴⁸S. J. Marrink and D. P. Tieleman, *Chem. Soc. Rev.* **42**, 6801 (2013).
- ⁴⁹D. H. de Jong, S. Baoukina, H. I. Ingólfsson, and S. J. Marrink, *Comput. Phys. Commun.* **199**, 1 (2016).
- ⁵⁰M. Parrinello and A. Rahman, *J. Appl. Phys.* **52**, 7182 (1981).
- ⁵¹G. Bussi, D. Donadio, and M. Parrinello, *J. Chem. Phys.* **126**, 014101 (2007).
- ⁵²M. J. Abraham, T. Murtola, R. Schulz, S. Páll, J. C. Smith, B. Hess, and E. Lindahl, *SoftwareX* **1-2**, 19 (2015).
- ⁵³S. Páll, A. Zhmurov, P. Bauer, M. Abraham, M. Lundborg, A. Gray, B. Hess, and E. Lindahl, *J. Chem. Phys.* **153**, 134110 (2020).
- ⁵⁴A. Sharma, V. V. Tyagi, C. R. Chen, and D. Buddhi, *Renewable and Sustainable Energy Rev.* **13**, 318 (2009).
- ⁵⁵V. M. Nazarychev, A. D. Glova, S. V. Larin, A. V. Lyulin, S. V. Lyulin, and A. A. Gurtovenko, *Int. J. Mol. Sci.* **23**, 14576 (2022).
- ⁵⁶W. F. Seyer, R. F. Patterson, and J. L. Keays, *J. Am. Chem. Soc.* **66**, 179 (1944).
- ⁵⁷A. P. Shlosinger and E. W. Bentilla, "Research and development study on thermal control by use of fusible materials," NASA Technical Report No. NASA-CR-67695, 1965.
- ⁵⁸A. D. Glova, I. V. Volgin, V. M. Nazarychev, S. V. Larin, S. V. Lyulin, and A. A. Gurtovenko, *RSC Adv.* **9**, 38834 (2019).
- ⁵⁹I. V. Volgin, A. D. Glova, V. M. Nazarychev, S. V. Larin, S. V. Lyulin, and A. A. Gurtovenko, *RSC Adv.* **10**, 31316 (2020).
- ⁶⁰K. M. Salerno, A. Agrawal, D. Perahia, and G. S. Grest, *Phys. Rev. Lett.* **116**, 058302 (2016).
- ⁶¹G. M. Torrie and J. P. Valleau, *J. Comput. Phys.* **23**, 187 (1977).
- ⁶²S. Kumar, J. M. Rosenberg, D. Bouzida, R. H. Swendsen, and P. A. Kollman, *J. Comput. Chem.* **13**, 1011 (1992).
- ⁶³J. S. Hub, B. L. de Groot, and D. van der Spoel, *J. Chem. Theory Comput.* **6**, 3713 (2010).
- ⁶⁴J. Wang, R. M. Wolf, J. W. Caldwell, P. A. Kollman, and D. A. Case, *J. Comput. Chem.* **25**, 1157 (2004).
- ⁶⁵J. B. Klauda, R. M. Venable, J. A. Freites, J. W. O'Connor, D. J. Tobias, C. Mondragon-Ramirez, I. Vorobyov, A. D. MacKerell, and R. W. Pastor, *J. Phys. Chem. B* **114**, 7830 (2010).
- ⁶⁶J. B. Klauda, B. R. Brooks, A. D. MacKerell, R. M. Venable, and R. W. Pastor, *J. Phys. Chem. B* **109**, 5300 (2005).
- ⁶⁷U. Essmann, L. Perera, M. L. Berkowitz, T. Darden, H. Lee, and L. G. Pedersen, *J. Chem. Phys.* **103**, 8577 (1995).
- ⁶⁸B. Hess, *J. Chem. Theory Comput.* **4**, 116 (2008).
- ⁶⁹S. Nose, *Mol. Phys.* **52**, 255 (1984).
- ⁷⁰W. G. Hoover, *Phys. Rev. A* **31**, 1695 (1985).
- ⁷¹B. Dünweg and K. Kremer, *Phys. Rev. Lett.* **66**, 2996 (1991).
- ⁷²B. Dünweg and K. Kremer, *J. Chem. Phys.* **99**, 6983 (1993).
- ⁷³I.-C. Yeh and G. Hummer, *J. Phys. Chem. B* **108**, 15873 (2004).
- ⁷⁴P. H. Gross and H. K. Zimmerman, *Rheol. Acta* **3**, 290 (1964).